PHYSICAL REVIEW B **89**, 241106(R) (2014)

Resonating-valence-bond superconductors with fermionic projected entangled pair states

Didier Poilblanc,[1] Philippe Corboz,[2,3] Norbert Schuch,[4] and J. Ignacio Cirac[5]
[1]*Laboratoire de Physique Théorique, C.N.R.S. and Université de Toulouse, 31062 Toulouse, France*
[2]*Theoretische Physik, ETH-Zurich, 8093 Zurich, Switzerland*
[3]*Institute for Theoretical Physics, University of Amsterdam, Science Park 904 Postbus 94485, 1090 GL Amsterdam, The Netherlands*
[4]*Institut für Quanteninformation, RWTH Aachen, D-52056 Aachen, Germany*
[5]*Max-Planck-Institut für Quantenoptik, Hans-Kopfermann-Straße 1, D-85748 Garching, Germany*
(Received 1 May 2014; revised manuscript received 13 June 2014; published 27 June 2014)

We construct a family of simple fermionic projected entangled pair states (fPEPS) on the square lattice with bond dimension $D = 3$ which are exactly hole-doped resonating valence bond (RVB) wave functions with short-range singlet bonds. Under doping the insulating RVB spin liquid evolves immediately into a superconductor with mixed $d + is$ pairing symmetry whose pair amplitude grows as the square root of the doping. The relative weight between s-wave and d-wave components can be controlled by a single variational parameter c. We optimize our ansatz with respect to c for the frustrated t-J_1-J_2 model (including both nearest and next-nearest neighbor antiferromagnetic interactions J_1 and J_2, respectively) for $J_2 \simeq J_1/2$ and obtain an energy very close to the infinite-PEPS state (using full update optimization and same bond dimension). The orbital symmetry of the optimized RVB superconductor has predominant d-wave character, although we argue a residual (complex s-wave) time reversal symmetry breaking component should always be present. Connections of the results to the physics of superconducting cuprates and pnictides are outlined.

DOI: 10.1103/PhysRevB.89.241106 PACS number(s): 75.10.Kt, 75.10.Jm

Introduction. The concept of the resonant valence bond (RVB) state was first introduced by Anderson [1] to describe a possible quantum disordered ground state in the triangular lattice $S = 1/2$ Heisenberg antiferromagnet. Insulating RVB states are commonly defined as equal weight superpositions of hard-core coverings of nearest-neighbor (NN) or short-range singlets. Such RVB states are now well understood thanks to a large variety of large-scale approaches such as the improved Monte Carlo sampling scheme for valence bonds, the use of representations in terms of simple projected entangled pair states (PEPS), or mapping into projected BCS wave functions; while the RVB state on the square lattice is critical [2–4] their analogs on kagome and triangular lattices were shown [5–8] to be $\mathbb{Z}_2$ gapped spin liquids. Interestingly, recent numerical results pointed towards an algebraic spin liquid in the frustrated spin-1/2 J_1-J_2 antiferromagnetic (AFM) Heisenberg model on the square lattice [4], which might also be the sign of a critical point between a Néel AFM state and a dimer state [9].

The RVB ideas have naturally been extended away from the 1/2-filled Mott insulator at electron density $n < 1$, and a "RVB superconductor" has been proposed as a simple mechanism in the high-temperature cuprate superconductors [10,11]. However, neutron scattering [12], scanning tunneling microscopy [13], nuclear magnetic resonance [14], and resonant soft x-ray scattering [15] experiments have shown that the cuprate parent AFM phase (generically) evolves under doping into complex intertwined phases involving, e.g., charge-stripe or nematic orders. As suggested in Fig. 1(a) (quantum disordered) RVB spin liquid stabilized by magnetic frustration would however have a more straightforward evolution under doping. Nevertheless, little is known about RVB states in which charge fermionic degrees of freedom come into play, although preliminary work has been done on (fermionic) doped dimer liquids lacking spin-SU(2) symmetry [16,17]. In this Rapid Communication, we introduce a general *fermionic* doped RVB state written as a $D = 3$ projected entangled paired state (PEPS) on the square lattice. This state is obtained by (i) rewriting the nearest-neighbor RVB PEPS [4–6] *in the fermion representation*, (ii) introducing vacant sites corresponding to a finite (average) density $x = 1 - n$ of doped holes (or "holons"), and finally, (iii) introducing longer range singlets (e.g., along diagonal bonds) *next* to some of the doped holes in a way that meets all lattice symmetries. Step (iii) is controlled by a single variational parameter c. We show that this state is a superconductor [hence breaking charge $U(1)$ symmetry] which (generically) inherits the mixed $d + is$ orbital symmetry of its parent (insulating) spin liquid, although its s-wave component is severely suppressed by (iii). Optimizing the hole kinetic energy with respect to c we obtain a good ansatz for the fermionic hole-doped frustrated spin-1/2 J_1-J_2 AFM Heisenberg model at $J_2 = 0.5J_1$ and $J_1 = 0.4t$ (the so-called t-J_1-J_2 model). The idea is therefore to introduce a simple yet competing wave function that enables us to understand unconventional superconducting ground states of strongly correlated fermions.

Doped RVB states in PEPS formalism. In the PEPS with bond dimension $D = 3$ we consider, each physical site has 4 virtual spins attached, each of which spans a virtual dimension of spin $1/2 \oplus 0$. On every bond, every pair of the NN virtual spins is projected to a virtual spin singlet state, $|\mathcal{S}\rangle = |01\rangle - |10\rangle + |22\rangle$, where the virtual indices "0,1" span the subspace of spin-1/2 and virtual index "2" spans the subspace of spin-0 [18]. At each site, one considers a projector $\mathcal{P}$ to enforce the local physical degrees of freedom. Finally, contracting the virtual index of each $\mathcal{S}$ at the bond and each $\mathcal{P}$ at the vertex yields the desired PEPS state.

We start with $\mathcal{P} = \mathcal{P}_0$ which maps one of the virtual spin-1/2 subspaces onto the physical spin-1/2 state (leaving the rest of virtual spins in the "2" state) and gives exactly the equal weight NN RVB state of Fig. 2(a) [5,6]. Next, a fermionic character is assigned to both virtual and physical spins-1/2 following the procedure of Ref. [19] to construct a fermionic

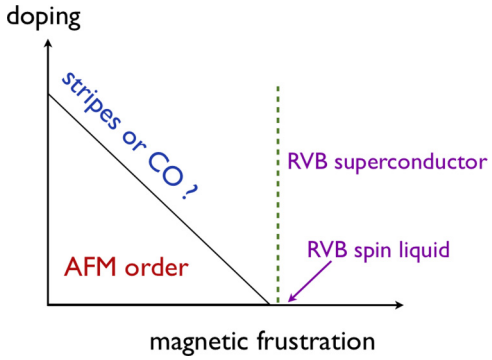

FIG. 1. (Color online) Schematic ($T = 0$) phase diagram of an AFM Mott insulator as a function of doping and magnetic frustration. Doping the AFM phase might involve complex phases such as "stripes" or charge ordered (CO) states. If a RVB liquid is stabilized by magnetic frustration it would evolve naturally under doping (dotted line) into a RVB superconductor.

PEPS (fPEPS). To recover the previous bosonic RVB state one must now include an extra i complex factor on (let us say) the vertical singlets, i.e., $|\mathcal{S}\rangle = i(|01\rangle - |10\rangle) + |22\rangle$, leading to $d + is$ point group (or orbital) symmetry [20]. One can now dope the fermonic $d + is$ RVB insulator by simply enlarging the physical space to vacant sites labeled, e.g., by the index "2". Adding a projector $\mathcal{P}_1$ enforcing all (both virtual and physical) spins in the "2" state generates local hole configurations labeled by "1" in Figs. 2(b)–2(d). However, the doped RVB state characterized only by $\mathcal{P} = \mathcal{P}_0 + \lambda\mathcal{P}_1$ (where λ plays the role of a "chemical potential") has zero expectation value of the hole kinetic operator between NN sites,

$$H_K = -t \sum_{\langle ij \rangle} P_G \, c^\dagger_{i,\sigma} c_{j,\sigma} \, P_G + \text{H.c.}, \tag{1}$$

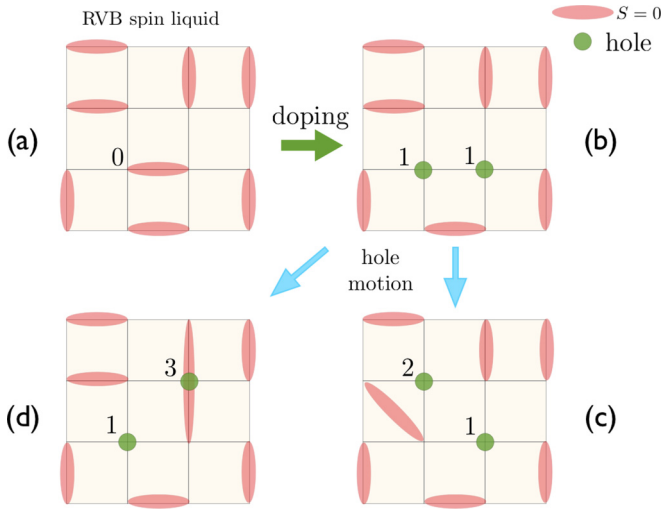

FIG. 2. (Color online) (a)–(d) Red segments represent singlet pairs of *physical* spin-1/2s. Green dots represent doped holes which can hop in the x or y directions. In the RVB insulator (a) or superconductor (b)–(d), *resonances* between many such configurations occur. fPEPS tensor elements encode each of the site configurations labeled from 0 to 3.

where $c^\dagger_{i,\sigma}$ creates a fermion (electron) of spin σ at site i and P_G is the Gutzwiller projector enforcing the physical Hilbert space that excludes doubly occupied sites, and therefore cannot be a physical representation of doped Mott insulators. To circumvent such a problem we allow singlet pairings between sites on the *same sublattice* in the immediate vicinity of some holes, as, e.g., holes "2" and "3" in Fig. 2(c) and Fig. 2(d), respectively. This can be achieved by extending the idea of Ref. [4] to the doped case and using a "teleportation" projector,

$$\mathcal{P}_2 = \sum_{i \neq j \neq k \neq l} |2\rangle\langle 22|_{ij} \otimes \langle \epsilon|_{kl}, \tag{2}$$

where $|\epsilon\rangle_{kl}$ is a singlet between sites k and l at distance $\sqrt{2}$ (choosing an anticlockwise orientation around the hole) or 2 (oriented from left to right, bottom to top). A general doped RVB wave function is a parameter c weighted combination of projectors $\mathcal{P} \equiv \mathcal{P}_0 + \lambda(\mathcal{P}_1 + c\mathcal{P}_2)$ at each vertex ($\lambda \in \mathbb{C}$, $c \in \mathbb{R}$) traced out with the bond singlets $\mathcal{S}$ at each bond and including the fermion signs according to Ref. [19]. Note that this RVB wave function is defined in the *grand-canonical* ensemble with fluctuating particle number.

Superconducting order. Using λ to tune the hole density x, we have investigated the properties of this one-parameter RVB family on an infinitely long cylinder with a circumference of $N_v = 6$ unit cells. As soon as $c \neq 0$, $\langle H_K \rangle \neq 0$ as shown in Fig. 3(a). A kinetic energy per hole $\langle H_K \rangle / x$ as large as $\sim -2.5t$ can be obtained for $c \simeq -0.65$ (when $x \to 0$).

By construction the doped RVB ansatz breaks the charge $U(1)$ symmetry. This is reflected by finite superconducting (SC) (singlet) pairings $\Delta_{ij} \equiv \langle c_{i,\uparrow} c_{j,\downarrow} \rangle$ for any finite doping x. Changing the phase of λ changes the (global) phase of the SC order parameter; i.e., $\lambda \to \exp(i\phi)\lambda$ leads to $\Delta_{ij} \to \exp(2i\phi)\Delta_{ij}$. The SC amplitude $|\Delta_{ij}|$ is largest when i and j are NN sites. Note that the NN pairings Δ_X and Δ_Y along the horizontal and vertical directions, respectively, differ slightly because of the finite cylinder circumference. Their average amplitude $\frac{1}{2}(|\Delta_X| + |\Delta_Y|)$ plotted in Fig. 3(b) shows that Δ_{ij} grows like $\sqrt{x}$.

We now examine the orbital symmetry of the NN pairing field that we decompose into its (*a priori* complex) s- and d-wave components, $\Delta_{\text{sw}} = \frac{1}{2}(\Delta_X + \Delta_Y)$ and $\Delta_{\text{dw}} = \frac{1}{2}(\Delta_X - \Delta_Y)$, respectively. We define the ratio $R = \Delta_{\text{sw}}/\Delta_{\text{dw}} = |R| \exp(i\Psi)$ and plot its amplitude $|R|$ and phase Ψ in Fig. 3(c) and Fig. 3(d), respectively. Note that only the *relative* phase Ψ between the Δ_{sw} and Δ_{dw} components matters since the overall SC phase can be changed by changing the phase of λ. First, we find that Ψ is almost exactly $\pi/2$—as expected for $d + is$ orbital symmetry. For $c = 0$ the RVB superconductor is a pure NN $d + is$ superconductor with exactly the same s- and d-wave amplitudes. The s-wave component is suppressed by increasing the parameter c, as the single hole kinetic energy increases (in magnitude). Interestingly, weak pairing between next-nearest neighbor (NNN) sites (i.e., along the plaquette diagonals) develops for increasing c, as shown in Figs. 3(b) and 3(c). The NNN pairing has s-wave orbital symmetry and, as the NN s-wave component, a relative phase of $\sim\pi/2$ with respect to the leading NN d-wave component, as shown in Fig. 3(d). The superconducting coherence length which is, strictly speaking, of one lattice spacing for $c = 0$ (the NNN

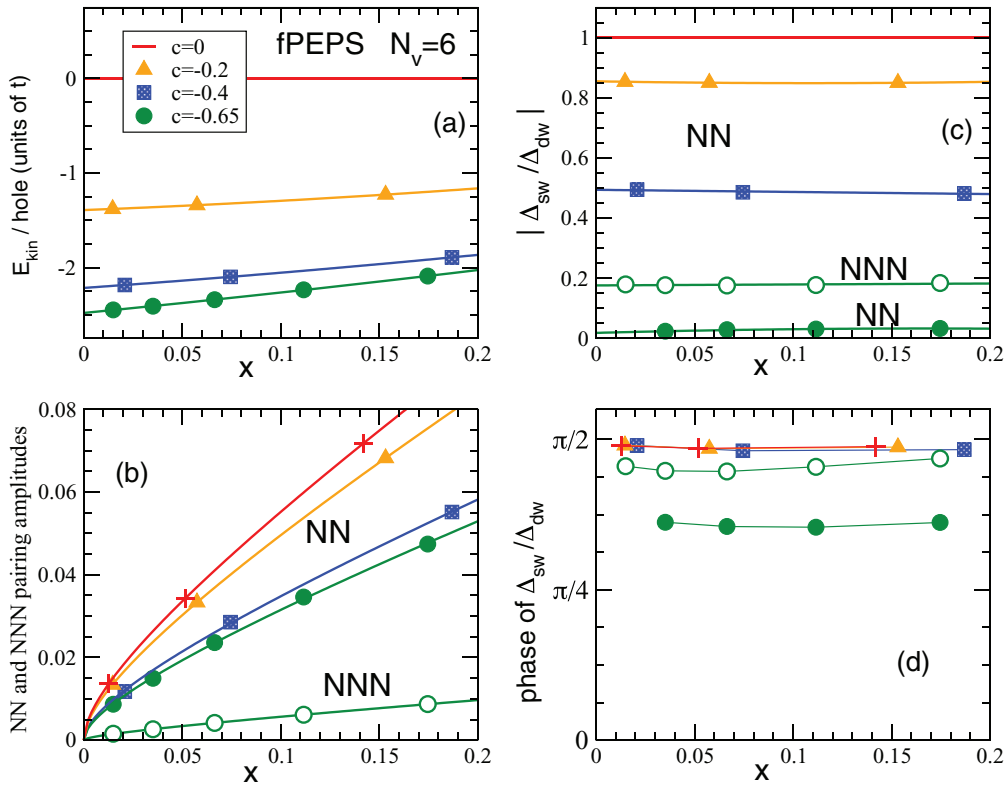

FIG. 3. (Color online) Hole kinetic energy (a) and NN pairings (b)–(d) of the RVB superconductor vs doping, for several values of the parameter c, computed on an infinite $N_v = 6$ cylinder. For $c = -0.65$, data for the (s-wave) NNN pairing are also shown (open symbols). Ratio of the amplitudes (c) and relative phase (d) between the s-wave and the NN d-wave components. $c = 0$ is a NN pure $d + is$ superconductor with zero kinetic energy (red lines).

pairing vanishes) grows for increasing c, yielding to a strong decrease of the NN Coulomb repulsion [21] (together with a gain of kinetic energy).

Optimized RVB superconductor. With the schematic phase diagram of Fig. 1 in mind, we now introduce the "frustrated t-J model,"

$$H = H_K + J_1 \sum_{\langle ij \rangle} \mathbf{S}_i \cdot \mathbf{S}_j + J_2 \sum_{\langle\langle kl \rangle\rangle} \mathbf{S}_k \cdot \mathbf{S}_l, \qquad (3)$$

involving AFM interactions J_1 and J_2 between NN and NNN sites, respectively. For $J_2 = 0$, recent infinite-PEPS (iPEPS) calculations [22] revealed an extremely close competition between a uniform d-wave superconducting state and different stripe states under doping the Néel AFM insulator. Here, we instead fix $J_2 = 0.5J_1$ for which we expect the half-filled GS to be a critical spin liquid well approximated by the simple NN RVB [4] discussed above. Therefore, at finite hole density, the doped (fermionic) $d + is$ RVB state naturally becomes a promising variational candidate for Hamiltonian (3). We find that the amplitude $|\langle H_K \rangle|$ in this state of the kinetic energy is maximized for $c \simeq -0.65$, and the corresponding data are shown in Fig. 4(a). A crude fit gives that the kinetic energy per hole behaves as $e_k \simeq (-2.5 + 2.3x)t$. On the other hand, mobile holes, by perturbing the spin RVB background, cost magnetic energy that is balancing the gain of kinetic energy. The magnetic energy cost (per hole) can be quantitatively defined as $e_m = (|\langle H_m \rangle_x| - |\langle H_m \rangle_0|)/x$, where $H_m = H - H_K$ is the magnetic part of (3) and $\langle \cdots \rangle_x$ is the expectation value in the RVB state at (average) doping x. A crude fit based on Fig. 4(b) gives $e_m \simeq (0.8 - 0.3x)J_1$ for $J_2 = 0.5J_1$. The overall total energy $\langle H_m \rangle_0 / N_s + x(e_k + e_m)$, normalized by the number of sites N_s, is shown in Fig. 4(c) and the hole contribution $e_k + e_m$ in Fig. 4(d), assuming $J_1 = 0.4t$. Note that the largest density correlation occurs between NNN sites [21] suggesting that Cooper pairs are predominantly NNN hole pairs despite the dominant d-wave character of the pairing field, in agreement with early numerics [23].

We have compared in Figs. 4(a)–4(d) the results for the constructed RVB state to iPEPS calculations using a 4-site unit cell, "simple" [24] and "full" update [25] schemes, and the same bond dimension $D = 3$ [21]. As seen in Fig. 4(c), the total energy of the $d + is$ RVB is very close to the optimized iPEPS energy (starting from a random configuration and full update). In fact, using the local tensor of the RVB state as a starting point, only minor improvement is obtained with the iPEPS optimization scheme. The $d + is$ RVB state is therefore a very good variational ansatz.

Discussion. Although magnetic frustration is weak in the high-temperature cuprate superconductors [26,27], it certainly plays an important role in the iron pnictide superconductors for which a frustrated Heisenberg model has been proposed [28,29], despite the multiorbital character of the materials. In any case, the uniform RVB superconductor we propose here might extend to a larger region of the phase diagram of Fig. 1 than just the dotted line (corresponding to the present work) and might have some relevance to the physics of

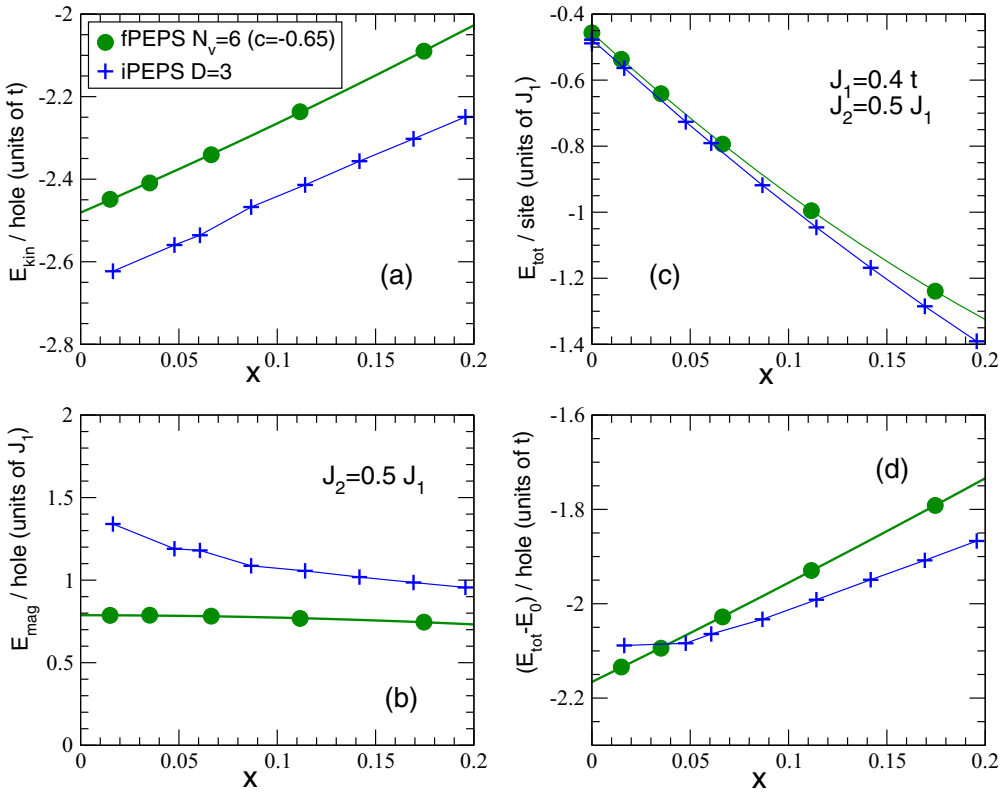

FIG. 4. (Color online) (a)–(d) Variational energies of the RVB superconductor (with $c = -0.65$) as a function of doping x. (a) Kinetic energy per hole; (b) magnetic energy cost per hole; total energy per site (c) and per hole (subtracting the $x = 0$ contribution) (d). Comparisons with the $D = 3$ iPEPS state optimized using the full update scheme (crosses) are shown.

high-temperature superconducting materials. At finite temperature, superconducting phase coherence may be lost while singlet pairing still occurs, hence providing a simple picture for the "pseudogap phase" of the cuprates. Interestingly, our scenario predicts a small residual *imaginary* s-wave component of the pairing field (at zero temperature) which would give rise to (very weak) broken time reversal symmetry (BTRS). Note that early claims of BTRS were made in the cuprates based on angular resolved photoemission (ARPES) experiments [30] but recent polar Kerr-effect measurements [31] have been interpreted in terms of chiral charge ordering. Incidentally, no orbital currents—as suggested by polarized neutron diffraction experiments [32]—occur in our RVB superconductor.

Acknowledgments. D.P. acknowledges the NQPTP ANR-0406-01 grant (French Research Council) for support. The computational results presented have been achieved using the CALMIP Hyperion Cluster (Toulouse). N.S. acknowledges support from the Alexander von Humboldt Foundation. I.C. acknowledges support from the EU project SIQS.

[1] P. W. Anderson, Mat. Res. Bull. **8**, 153 (1973).
[2] A. F. Albuquerque and F. Alet, Phys. Rev. B **82**, 180408(R) (2010).
[3] Y. Tang, A. W. Sandvik, and C. L. Henley, Phys. Rev. B **84**, 174427 (2011).
[4] Ling Wang, Didier Poilblanc, Zheng-Cheng Gu, Xiao-Gang Wen, and Frank Verstraete, Phys. Rev. Lett. **111**, 037202 (2013).
[5] N. Schuch, D. Poilblanc, J. I. Cirac, and D. Perez-Garcia, Phys. Rev. B **86**, 115108 (2012).
[6] D. Poilblanc, N. Schuch, D. Perez-Garcia, and J. I. Cirac, Phys. Rev. B **86**, 014404 (2012).
[7] J. Wildeboer and A. Seidel, Phys. Rev. Lett. **109**, 147208 (2012).
[8] F. Yang and H. Yao, Phys. Rev. Lett. **109**, 147209 (2012).
[9] A. Sandvik, Phys. Rev. B **85**, 134407 (2012).
[10] P. W. Anderson, Science **235**, 1196 (1987).
[11] P. A. Lee, Naoto Nagaosa, and X.-G. Wen, Rev. Mod. Phys. **78**, 17 (2006).
[12] J. M. Tranquada, B. J. Sternlieb, J. D. Axe, Y. Nakamura, and S. Uchida, Nature (London) **375**, 561 (1995).
[13] M. J. Lawler, K. Fujita, Jhinhwan Lee, A. R. Schmidt, Y. Kohsaka, Chung Koo Kim, H. Eisaki, S. Uchida, J. C. Davis, J. P. Sethna, and Eun-Ah Kim, Nature (London) **466**, 374 (2010).
[14] Tao Wu, Hadrien Mayaffre, Steffen Krämer, Mladen Horvatic, Claude Berthier, W. N. Hardy, Ruixing Liang, D. A. Bonn, M.-H. Julien, and Marc-Henri Julien, Nature (London) **477**, 191 (2011).
[15] P. Abbamonte, E. Demler, J. C. S. Davis, and J.-C. Campuzano, Physica C **481**, 15 (2012).
[16] D. Poilblanc, Phys. Rev. Lett. **100**, 157206 (2008).
[17] C. A. Lamas, A. Ralko, M. Oshikawa, D. Poilblanc, and P. Pujol, Phys. Rev. B **87**, 104512 (2013).

[18] To guarantee full translational invariance, singlets are oriented from left to right, bottom to top. At $x = 0$, this is equivalent to orienting them from one sublattice to the other, up to the insertion of a single vison line in the cylinder [4,6].

[19] Philippe Corboz, Roman Orus, Bela Bauer, and Guifre Vidal, Phys. Rev. B **81**, 165104 (2010).

[20] G. Kotliar, Phys. Rev. B **37**, 3664 (1988).

[21] See Supplemental Material at http://link.aps.org/supplemental/10.1103/PhysRevB.89.241106 which includes results on the density-density correlations in the RVB superconductors and details on the iPEPS calculations.

[22] Philippe Corboz, T. M. Rice, and Matthias Troyer, arXiv:1402.2859.

[23] D. Poilblanc, Phys. Rev. B **49**, 1477 (1994).

[24] Philippe Corboz, Jacob Jordan, and Guifré Vidal, Phys. Rev. B **82**, 245119 (2010).

[25] Philippe Corboz and Frédéric Mila, Phys. Rev. B **87**, 115144 (2013).

[26] R. Coldea, S. M. Hayden, G. Aeppli, T. G. Perring, C. D. Frost, T. E. Mason, S.-W. Cheong, and Z. Fisk, Phys. Rev. Lett. **86**, 5377 (2001).

[27] Carmen J. Calzado and Jean-Paul Malrieu, Phys. Rev. B **63**, 214520 (2001).

[28] Dao-Xin Yao and E. W. Carlson, Phys. Rev. B **78**, 052507 (2008).

[29] Pallab Goswami, Rong Yu, Qimiao Si, and Elihu Abrahams, Phys. Rev. B **84**, 155108 (2011).

[30] A. Kaminski, S. Rosenkranz, H. M. Fretwell, J. C. Campuzano, Z. Li, H. Raffy, W. G. Cullen, H. You, C. G. Olson, C. M. Varma and H. Höchst, Nature (London) **416**, 610 (2002).

[31] Hovnatan Karapetyan, Jing Xia, M. Hucker, G. D. Gu, J. M. Tranquada, M. M. Fejer, and A. Kapitulnik, Phys. Rev. Lett. **112**, 047003 (2014).

[32] B. Fauqué, Y. Sidis, V. Hinkov, S. Pailhès, C. T. Lin, X. Chaud, and P. Bourges, Phys. Rev. Lett. **96**, 197001 (2006).